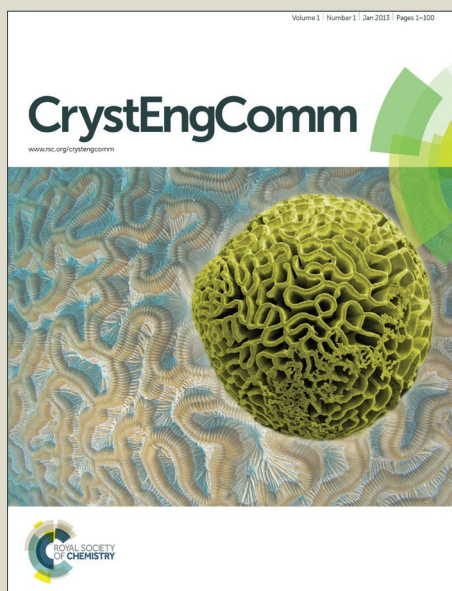


CrystEngComm

Accepted Manuscript



This is an *Accepted Manuscript*, which has been through the Royal Society of Chemistry peer review process and has been accepted for publication.

Accepted Manuscripts are published online shortly after acceptance, before technical editing, formatting and proof reading. Using this free service, authors can make their results available to the community, in citable form, before we publish the edited article. We will replace this *Accepted Manuscript* with the edited and formatted *Advance Article* as soon as it is available.

You can find more information about *Accepted Manuscripts* in the [Information for Authors](#).

Please note that technical editing may introduce minor changes to the text and/or graphics, which may alter content. The journal's standard [Terms & Conditions](#) and the [Ethical guidelines](#) still apply. In no event shall the Royal Society of Chemistry be held responsible for any errors or omissions in this *Accepted Manuscript* or any consequences arising from the use of any information it contains.

Counter-ion control of structure in uranyl ion complexes with 2,5-thiophenedicarboxylate†

Pierre Thuéry^a and Jack Harrowfield^b

^a NIMBE, CEA, CNRS, Université Paris-Saclay, CEA Saclay, 91191 Gif-sur-Yvette, France. E-mail:

pierre.thuery@cea.fr

^b ISIS, Université de Strasbourg, 8 allée Gaspard Monge, 67083 Strasbourg, France. E-mail:

harrowfield@unistra.fr

2,5-Thiophenedicarboxylic acid (H₂TDC) was reacted with uranyl nitrate under solvo-hydrothermal conditions with acetonitrile or *N*-methyl-2-pyrrolidone as organic co-solvents and different combinations of d-block metal ions and *N*-donating chelators. The complexes [Ni(bipy)₃][(UO₂)₂(TDC)₂(HTDC)(NO₃)]·NMP·H₂O (**1**) and [Co((NH₂)₂sar)]·[(UO₂)₂(TDC)₂(HTDC)₂]·Cl·6H₂O (**2**) (bipy = 2,2'-bipyridine, sar = sarcophagine = 3,6,10,13,16,19-hexaazabicyclo[6.6.6]icosane), the latter containing the enantiomerically pure Λ-isomer of the counter-ion, crystallize as one-dimensional coordination polymers in which the TDC²⁻ ligands are bis-chelating and the HTDC⁻ ones are mono-chelating and terminal. Two-dimensional (2D) honeycomb networks with all ligands bis-chelating are generated in the two isomorphous complexes [Fe(phen)₃]₂[(UO₂)₄(TDC)₆][UO₂(NMP)₂(NO₃)₂]·2NMP (**3**) and [Ni(phen)₃]₂[(UO₂)₄(TDC)₆][UO₂(NMP)₂(NO₃)₂]·NMP (**4**) (phen = 1,10-phenanthroline), while a 2D assembly with a tessellation of 4- and 8-membered rings (fes topological type) is formed in [Ag(CH₃CN)₃]₂[(UO₂)₂(TDC)₃]·H₂O (**5**). Finally, [Ag(bipy)₂]₅[(UO₂)₄(TDC)₆]·NO₃·6H₂O (**6**) comprises planar honeycomb networks which generate a three-dimensional (3D) architecture through inclined 2D → 3D polycatenation; the [Ag(bipy)₂]⁺ cations are assembled into columns held by π-stacking and weak argentophilic interactions, which occupy the channels formed by the intersecting layers. Complete quenching of uranyl luminescence occurs in complexes **1–4** and only **6** displays an emission spectrum in the solid state showing the usual well-resolved vibronic fine structure.

† CCDC reference numbers 1437894–1437899. For crystallographic data in CIF or other electronic format see DOI:

Introduction

In the search for ways of inducing variations in the geometries of the complexes, coordination polymers or frameworks¹ formed by uranyl ions with polycarboxylic acids,² the use of chiral counter-ions of the type $[\text{ML}_3]^{2+}$, where M is a d-block transition metal cation and L a chelating nitrogen donor, either 2,2'-bipyridine (bipy) or 1,10-phenanthroline (phen), has proven to be a valuable approach (as is, more generally, the use of such *N*-donors in the synthesis of metal-organic frameworks³). In particular, it has allowed the isolation of the first uranyl-containing triple-stranded helicates, in which the helicity results from a close association with the chiral counter-ion,⁴ and also, alongside other less remarkable species, of polycatenated two-dimensional (2D) networks.⁵ In order to investigate the effect of counterions containing d-block metal ions and bipy or phen donors with other polycarboxylic acid families, we have now turned to 2,5-thiophenedicarboxylic acid (H_2TDC). Although it has been frequently used as a ligand, with 214 of its complexes reported in the Cambridge Structural Database (CSD, Version 5.35)⁶ (among which 65 with lanthanide ions), 2,5-thiophenedicarboxylic acid is not commonly found as a ligand for uranyl ions. The first uranyl ion complexes to be reported were molecular dinuclear species containing TDC^{2-} bridges and additional terpyridine co-ligands,⁷ while three-dimensional (3D) frameworks were shown to form in the presence of coordinated *N*-methyl-2-pyrrolidone (NMP).⁸ Complexes containing $[\text{M}(\text{phen})_3]^{2+}$ counterions (M = Fe, Ni) were subsequently found to adopt a honeycomb 2D topology.⁹ A very recent contribution from Cahill's group describes the influence of bipy and several of its di- and tetra-methylated derivatives, and also that of tetrakis(2-pyridyl)pyrazine, on the nature of the complexes formed by TDC^{2-} .¹⁰ In this case, 1D and 2D assemblies were obtained, with the *N*-donor species being either coordinated or present as

a neutral guest or a counter-ion. In the absence of an *N*-donor, a parallel 2D → 2D polycatenated system is generated,¹⁰ which is one of the rare examples of network interpenetration in uranyl structural chemistry.^{5,11} In the present work, we have used combinations of d-block metal ions (Fe^{2+} , Co^{3+} , Ni^{2+} and Ag^+), *N*-donors (bipy, phen, diaminosarcophagine) and organic solvents (NMP, acetonitrile) to generate six novel uranyl ion complexes with TDC^{2-} which were characterized by their crystal structure and, in all but one case, their emission spectrum in the solid state. A particular objective of the present work was to compare cations of distinctly different character with regard to their possible interactions with uranyl-containing anions. Thus, $[\text{M}(\text{phen})_3]^{2+}$ ($\text{M} = \text{Fe}, \text{Ni}$) are members of a family of chiral cations known for their tendency to become involved in aromatic...aromatic interactions¹² and $\text{CH}\cdots\text{O}$ interactions,¹³ while Λ - $[\text{Co}((\text{NH}_3)_2\text{sar})]^{5+}$ is a member of another family of chiral cations capable of multiple NH-bond donor interactions which can be controlled both by substitution on the cage ligand and change of the bound metal ion.¹⁴ In contrast, $\text{Ag}(\text{I})$ is a cation characterized by its common adoption of coordination numbers as low as 3 or even 2,¹⁵ and thus could be anticipated to provide simpler and possibly even direct (involving the primary coordination sphere) links¹⁶ between anions although, in the event, direct links were not found in the present cases.

Experimental

Synthesis

Caution! Uranium is a radioactive and chemically toxic element, and uranium-containing samples must be handled with suitable care and protection.

$\text{UO}_2(\text{NO}_3)_2 \cdot 6\text{H}_2\text{O}$ (depleted uranium, R. P. Normapur, 99%), $\text{Ni}(\text{NO}_3)_2 \cdot 6\text{H}_2\text{O}$ and AgNO_3 were purchased from Prolabo, 2,2'-bipyridine (bipy) was from Fluka, and 2,5-thiophenedicarboxylic acid (H_2TDC) and 1,10-phenanthroline (phen) from Aldrich. Elemental analyses were performed by MEDAC Ltd. at Chobham, UK.

$[\text{Fe}(\text{phen})_3](\text{CF}_3\text{SO}_3)_2$, a known complex,¹⁷ was prepared simply by addition of diethylether to a solution of $[\text{Fe}(\text{H}_2\text{O})_6](\text{CF}_3\text{SO}_3)_2$ (Aldrich) and 1,10-phenanthroline in a 1:3 molar ratio in ethanol. Λ - $[\text{Co}((\text{NH}_3)_2\text{sar})]\text{Cl}_5 \cdot 2\text{H}_2\text{O}$ [$(\text{NH}_3)_2\text{sar}$ = diammoniosarcophagine = 1,8-diammonio-3,6,10,13,16,19-hexaazabicyclo[6.6.6]icosane] was prepared from Λ - $[\text{Co}(\text{en})_3]\text{Cl}_3 \cdot 3\text{H}_2\text{O}$ (en = ethylenediamine) as described elsewhere.¹⁸

$[\text{Ni}(\text{bipy})_3][(\text{UO}_2)_2(\text{TDC})_2(\text{HTDC})(\text{NO}_3)] \cdot \text{NMP} \cdot \text{H}_2\text{O}$ (**1**). H_2TDC (17 mg, 0.10 mmol), $\text{UO}_2(\text{NO}_3)_2 \cdot 6\text{H}_2\text{O}$ (50 mg, 0.10 mmol), $\text{Ni}(\text{NO}_3)_2 \cdot 6\text{H}_2\text{O}$ (29 mg, 0.10 mmol), 2,2'-bipyridine (47 mg, 0.30 mmol), *N*-methyl-2-pyrrolidone (NMP, 0.4 mL), and demineralized water (0.8 mL) were placed in a 15 mL tightly closed glass vessel and heated at 140 °C under autogenous pressure, giving light yellow crystals of complex **1** overnight (36 mg, 61% yield based on H_2TDC). Anal. calcd for $\text{C}_{53}\text{H}_{42}\text{N}_8\text{NiO}_{21}\text{S}_3\text{U}_2$: C, 36.21; H, 2.41; N, 6.37; S, 5.47. Found: C, 36.95; H, 2.45; N, 6.58; S, 5.71%.

$[\text{Co}((\text{NH}_2)_2\text{sar})][(\text{UO}_2)_2(\text{TDC})_2(\text{HTDC})_2] \cdot \text{Cl} \cdot 6\text{H}_2\text{O}$ (**2**). H_2TDC (17 mg, 0.10 mmol), $\text{UO}_2(\text{NO}_3)_2 \cdot 6\text{H}_2\text{O}$ (50 mg, 0.10 mmol), Λ - $[\text{Co}((\text{NH}_3)_2\text{sar})]\text{Cl}_5 \cdot 2\text{H}_2\text{O}$ (30 mg, 0.05 mmol), acetonitrile (0.4 mL), and demineralized water (0.8 mL) were placed in a 15 mL tightly closed glass vessel and heated at 140 °C under autogenous pressure, giving light yellow crystals of complex **2** within five days (14 mg, 32% yield based on H_2TDC). Anal. calcd for $\text{C}_{38}\text{H}_{56}\text{ClCoN}_8\text{O}_{26}\text{S}_4\text{U}_2$: C, 26.24; H, 3.24; N, 6.44. Found: C, 26.25; H, 3.07; N, 6.27%.

$[\text{Fe}(\text{phen})_3]_2[(\text{UO}_2)_4(\text{TDC})_6][\text{UO}_2(\text{NMP})_2(\text{NO}_3)_2] \cdot 2\text{NMP}$ (**3**). H_2TDC (17 mg, 0.10 mmol), $\text{UO}_2(\text{NO}_3)_2 \cdot 6\text{H}_2\text{O}$ (50 mg, 0.10 mmol), $[\text{Fe}(\text{phen})_3](\text{CF}_3\text{SO}_3)_2$ (22 mg, 0.025 mmol), NMP (0.3 mL), and demineralized water (0.5 mL) were placed in a 15 mL tightly closed glass vessel and heated at 140 °C under autogenous pressure, giving light yellow crystals of complex **3** overnight (21 mg, 41% yield based on Fe). Anal. calcd for $\text{C}_{128}\text{H}_{96}\text{Fe}_2\text{N}_{18}\text{O}_{44}\text{S}_6\text{U}_5$: C, 37.64; H, 2.37; N, 6.17. Found: C, 37.75; H, 2.35; N, 5.83%.

$[\text{Ni}(\text{phen})_3]_2[(\text{UO}_2)_4(\text{TDC})_6][\text{UO}_2(\text{NMP})_2(\text{NO}_3)_2] \cdot \text{NMP}$ (**4**). H_2TDC (17 mg, 0.10 mmol), $\text{UO}_2(\text{NO}_3)_2 \cdot 6\text{H}_2\text{O}$ (50 mg, 0.10 mmol), $\text{Ni}(\text{NO}_3)_2 \cdot 6\text{H}_2\text{O}$ (29 mg, 0.10 mmol), 1,10-phenanthroline (54 mg, 0.30 mmol), NMP (0.3 mL), and demineralized water (0.7 mL) were placed in a 15 mL tightly closed glass vessel and heated at 140 °C under autogenous pressure, giving light yellow crystals of complex **4** overnight (35 mg, 53% yield based on H_2TDC). Anal. calcd for $\text{C}_{123}\text{H}_{87}\text{N}_{17}\text{Ni}_2\text{O}_{43}\text{S}_6\text{U}_5$: C, 37.02; H, 2.20; N, 5.97. Found: C, 37.33; H, 2.31; N, 5.46%.

$[\text{Ag}(\text{CH}_3\text{CN})_3]_2[(\text{UO}_2)_2(\text{TDC})_3] \cdot \text{H}_2\text{O}$ (**5**). H_2TDC (17 mg, 0.10 mmol), $\text{UO}_2(\text{NO}_3)_2 \cdot 6\text{H}_2\text{O}$ (50 mg, 0.10 mmol), AgNO_3 (34 mg, 0.20 mmol), acetonitrile (0.3 mL), and demineralized water (0.8 mL) were placed in a 15 mL tightly closed glass vessel and heated at 140 °C under autogenous pressure, giving light yellow crystals of complex **5** in low yield within five days.

$[\text{Ag}(\text{bipy})_2]_5[(\text{UO}_2)_4(\text{TDC})_6] \cdot \text{NO}_3 \cdot 6\text{H}_2\text{O}$ (**6**). H_2TDC (17 mg, 0.10 mmol), $\text{UO}_2(\text{NO}_3)_2 \cdot 6\text{H}_2\text{O}$ (50 mg, 0.10 mmol), AgNO_3 (17 mg, 0.10 mmol), 2,2'-bipyridine (32 mg, 0.20 mmol), NMP (0.3 mL), and demineralized water (0.8 mL) were placed in a 15 mL tightly closed glass vessel and heated at 140 °C under autogenous pressure, giving light yellow crystals of complex **6** overnight (34 mg, 47% yield based on H_2TDC). The presence of about eight water molecules in excess of the number found from crystal structure determination is indicated by elemental analysis, in keeping with the presence of voids in the lattice (see below). Anal. calcd

for $C_{136}H_{104}Ag_5N_{21}O_{41}S_6U_4 + 8H_2O$: C, 36.17; H, 2.68; N, 6.51. Found: C, 36.13; H, 2.46; N, 6.50%.

Crystallography

The data were collected at 150(2) K on a Nonius Kappa-CCD area detector diffractometer¹⁹ using graphite-monochromated Mo $K\alpha$ radiation ($\lambda = 0.71073 \text{ \AA}$). The crystals were introduced into glass capillaries with a protective coating of Paratone-N oil (Hampton Research). The unit cell parameters were determined from ten frames, then refined on all data. The data (combinations of ϕ - and ω -scans with a minimum redundancy of at least 4 for 90% of the reflections) were processed with HKL2000.²⁰ Absorption effects were corrected empirically with the program SCALEPACK.²⁰ The structures were solved by intrinsic phasing with SHELXT,²¹ expanded by subsequent difference Fourier synthesis and refined by full-matrix least-squares on F^2 with SHELXL-2014.²² All non-hydrogen atoms were refined with anisotropic displacement parameters. Carbon-bound hydrogen atoms were introduced at calculated positions; all hydrogen atoms were treated as riding atoms with an isotropic displacement parameter equal to 1.2 times that of the parent atom (1.5 for CH_3 , with optimized geometry). Special details are as follows:

Compound 1. Restraints on bond lengths, angles and displacement parameters were applied for the atoms of the badly resolved NMP solvent molecule. The water solvent molecule is disordered over three positions close to one another, which have been given occupancy parameters of 0.33. The hydrogen atom bound to O15 was found on a difference Fourier map, but not those of the water molecules.

Compound 2. Two lattice water molecules were given occupancy factors of 0.5 in order to retain acceptable displacement parameters. Restraints on displacement parameters were applied

for three badly behaving oxygen atoms. The hydrogen atoms bound to N7, N8 and three water molecules were found on difference Fourier maps; those bound to N1–N6 were introduced at calculated positions. The refined value of the Flack parameter is $-0.005(9)$.

Compound 3. Restraints were applied on the displacement parameter of the methyl carbon atom of the solvent NMP molecule. The largest negative residual electron density peak is located near atom U3, as a result of imperfect absorption corrections and/or of unresolved disorder on this group, as suggested by the large displacement parameters of U3 and its ligands.

Compound 4. The NMP solvent molecule has been given an occupancy factor of 0.5 in order to retain acceptable displacement parameters. Restraints on bond lengths and displacement parameters were applied for the atoms of the solvent NMP molecule. The largest negative residual electron density peak is located near atom U3, as a result of imperfect absorption corrections and/or of unresolved disorder on this group, as suggested by the large displacement parameters of U3 and its ligands.

Compound 5. One dicarboxylate ligand is disordered over two mirror-related positions; only the two positions of the central ring are well resolved and an average position only was found for the atoms of the carboxylate group (notwithstanding their large and very anisotropic displacement parameters). One of the acetonitrile molecules bound to Ag1 is too close to its image by symmetry and was given an occupancy factor of 0.5 accordingly. The water solvent molecule was also given half-occupancy in order to retain an acceptable displacement parameter. Restraints on bond lengths were applied for the disordered acetonitrile molecule and restraints on displacement parameters for both acetonitrile molecules. The water hydrogen atoms were not found. Some voids in the lattice probably indicate the presence of other, unresolved solvent molecules.

Compound 6. Three aromatic rings were refined as idealized hexagons and restraints on bond lengths and displacement parameters were applied for several atoms, particularly in the bipy molecules and nitrate counter-ion. Several solvent water molecules were given occupancy factors of 0.5 in order to retain acceptable displacement parameters. The hydrogen atoms of three water molecules were found on a difference Fourier map. Some voids in the lattice likely indicate the presence of other, unresolved solvent molecules, in agreement with the elemental analysis results (see above). The refined value of the Flack parameter is 0.018(5).

Crystal data and structure refinement parameters are given in Table 1. The molecular plots were drawn with ORTEP-3²³ and the polyhedral representations with VESTA.²⁴ The topological analyses were made with TOPOS.²⁵

Luminescence measurements

Emission spectra were recorded on solid samples using a Horiba-Jobin-Yvon Fluorolog spectrofluorometer. The powdered complex was pressed between two silica plates which were mounted such that the faces were oriented vertically and at 45° to the incident excitation radiation. An excitation wavelength of 420 nm was used in all cases and the emissions monitored between 450 and 650 nm.

Results and discussion

Synthesis

Complexes 1–6 were synthesized under solvo-hydrothermal conditions at 140 °C (a value in the middle of the range of temperatures commonly employed). All crystals appeared during the

heating phase and their presence in the glass vials was checked visually. The organic solvents for which crystalline materials could be obtained were NMP for complexes **1**, **3**, **4** and **6**, and acetonitrile for **2** and **5**; these solvents are either absent from the final species (**2** and **6**) or present as ligands (**3**, **4**, **5**) and/or lattice guests (**1**, **3**, **4**). Previous results with other polycarboxylates have indicated that such solvo-hydrothermal conditions limit the formation of oxo/hydroxo-bridged uranyl secondary building units resulting from hydrolysis,^{8,26} and this is also observed here. It is notable that, although no base was added in the reaction medium, the dicarboxylate is fully deprotonated in all cases but for one uncoordinated acid group being retained in some of the ligands in both compounds **1** and **2**. The ammonio substituents of the cage ligand in the complex Λ -[Co((NH₃)₂sar)]⁵⁺ also undergo deprotonation in the formation of complex **2**. In the absence of a chelating *N*-donor, [Ag(CH₃CN)₃]⁺ ions are present in complex **5**.

Crystal Structures

The asymmetric unit in the complex [Ni(bipy)₃][(UO₂)₂(TDC)₂(HTDC)(NO₃)]·NMP·H₂O (**1**) contains two uranium atoms in different environments (Fig. 1). Both are in hexagonal bipyramidal environments but, while U2 is chelated by three carboxylate groups, one of the latter is replaced by a chelating nitrate ion in the case of U1. The U–O(carboxylate) bond lengths are in the range 2.422(4)–2.521(4) Å [average 2.47(3) Å] and are unexceptional, as are the U–O(nitrate) bond lengths of 2.496(4) and 2.528(4) Å. The two TDC²⁻ dicarboxylate ligands are doubly chelating, while the third HTDC⁻ ligand retains a carboxylic proton and chelates through only one of its functional groups. The coordination modes are thus mono- or bis-chelating, though monodentate and bridging bidentate bonding modes have previously been observed with this ligand and uranyl ions.^{7,8,10} Zigzag 1D coordination polymers directed along the [1 1 0] axis are

formed, with the sulfur atoms of the bridging ligands pointing in alternate directions and the nitrate ions and terminal HTDC⁻ ligands protruding on both edges. The carboxylic proton of the latter ligand, which has been found on the uncoordinated carboxyl unit, makes a hydrogen bond with the carbonyl oxygen atom of the solvent NMP molecule [O15...O20 2.599(6) Å, H...O20 1.64 Å, O15-H...O20 168°]. The dominant interactions ensuring crystal stability are coulombic in such an ionic species.²⁷ The TDC²⁻ ligand is of particular interest because of the functionality due to the thiophene ring and the possibility of its involvement in interactions of the sulfur centre such as the S... π ones found in protein crystal structures²⁸ or O...S/S...S chalcogen bonding,²⁹ although it is not expected to be a good donor site for metal ion coordination, and in fact analysis of the short contacts through calculation of the Hirshfeld surfaces³⁰ with CrystalExplorer 3.0³¹ indicates that the sulfur atom is not involved in interactions stronger than those of dispersion. The most prominent weak interactions between cation and anion are CH...O hydrogen bonds³² involving hydrogen atoms of the bipy molecules and either oxo, carboxylate or nitrate oxygen atoms, with H...O distances as short as 2.30 Å, as previously observed in other systems.^{4,33} Analysis of π -stacking contacts with PLATON³⁴ indicates that two parallel-displaced interactions may be present, one between the thiophene ring containing S1 and one bipy ring [centroid...centroid distance 4.123(4) Å, dihedral angle 8.7(3)°] and another between two bipy rings from different counter-ions [centroid...centroid distance 4.254(4) Å, slippage 2.52 Å].

Both enantiomers of the chiral [Ni(bipy)₃]²⁺ counter-ion are present as Δ, Λ pairs with a Ni...Ni separation of 9.2091(14) Å in **1**, which crystallizes in a centrosymmetric space group. In contrast, complex **2**, [Co((NH₂)₂sar)][(UO₂)₂(TDC)₂(HTDC)₂].Cl·6H₂O, was synthesized from the enantiomerically pure, externally protonated Λ -[Co((NH₃)₂sar)]⁵⁺ and it crystallizes in the

Sohncke group $P2_1$. As in complex **1**, the asymmetric unit contains two uranium atoms, both in hexagonal bipyramidal environments since they are chelated by three carboxylate groups (Fig. 2). Two of the four ligands are bis-chelating, doubly deprotonated bridges while the other two are terminal and retain one carboxylic proton. The main difference with **1** is thus the replacement of the nitrate ion by a terminal HTDC⁻ ligand. The U–O(carboxylate) bond lengths are in the range 2.435(9)–2.518(10) Å [average 2.48(2) Å], as usual. The zigzag ribbons formed are parallel to [1 0 $\bar{1}$] and they are nearly planar, with no conspicuous chirality induced by the counter-ions. As shown in Fig. 2, the presence of the protruding terminal ligands induces a bump-to-hollow arrangement of the chains in planes parallel to (1 0 1), with slight interdigitation. These sheets are arranged in groups of two, with the [Co((NH₂)₂sar)]³⁺ counter-ions located in between. When viewed down the normal to the (1 0 1) plane, these groups of two layers define cavities containing the counter-ions, while the chloride counter-ions are located between these groups of layers. Parallel-displaced π -stacking interactions may be present between thiophene rings pertaining to the two layers surrounding the [Co((NH₂)₂sar)]³⁺ counter-ions [centroid...centroid distance 3.951(8) Å, dihedral angle 9.2(7)° for the rings containing S1 and S3; centroid...centroid distance 3.789(8) Å, dihedral angle 2.2(7)° for the rings containing S2 and S4]. Hirshfeld surface analysis indicates that the main interactions present between the different components (apart from the electrostatic ones) are OH...O, OH...Cl, NH...O and NH...Cl hydrogen bonds which result in the formation of a 3D network. In particular, the [Co((NH₂)₂sar)]³⁺ counter-ions are held by two NH...O hydrogen bonds, one at each end, along the edge of the ribbons, as shown in Fig. 2 (they are also held via a solvent water molecule, not represented, which is an acceptor from N2 and N3 and is probably a donor to O5 and O14, although its hydrogen atoms were not found). The full hydrogen bonding capacity of the cation is not exploited in its interactions with the uranyl

polymer since the *lel*₃ conformation of the cage ligand is associated, as in many salts of the cation,¹⁴ with pairwise NH-bond chelation of small species, here two water molecules and a chloride ion. There are, however, various approaches of methylene-CH atoms to uranyl-bound oxygen atoms which indicate some parallel with the other cations studied in the present work.

The complexes $[M(\text{phen})_3]_2[(\text{UO}_2)_4(\text{TDC})_6][\text{UO}_2(\text{NMP})_2(\text{NO}_3)_2] \cdot x\text{NMP}$ ($M = \text{Fe}$, $x = 2$: **3**; $M = \text{Ni}$, $x = 1$: **4**) are isomorphous, the difference in the number of free NMP molecules possibly reflecting some desolvation of the crystals of **4**. They crystallize with unit cell parameters very close to those of one of the complexes previously described, $[\text{Fe}(\text{phen})_3][(\text{UO}_2)_2(\text{TDC})_3] \cdot \text{H}_2\text{TDC} \cdot 6\text{H}_2\text{O}$,⁹ and in the same space group, but the structures are nevertheless significantly distinct. The asymmetric unit in **3** and **4** contains three uranium atoms, one of them (U3) on an inversion centre. As shown in Fig. 3, U1 and U2 are both chelated by three carboxylate groups, while U3 is chelated by two nitrate ions and bound to two NMP molecules in trans positions to form a badly resolved, centrosymmetric neutral $[\text{UO}_2(\text{NMP})_2(\text{NO}_3)_2]$ unit (which replaces the probably protonated H_2TDC molecule in the previously reported compound). The U–O(carboxylate) bond lengths are in the range 2.436(6)–2.531(6) Å [average 2.48(2) Å] (including both compounds). In contrast to compounds **1** and **2**, all three TDC^{2-} ligands are bis-chelating, so that a 2D assembly parallel to the (1 1 1) plane is formed, which has the honeycomb (hcb) topology, with the point (Schläfli) symbol $\{6^3\}$. The six sulfur atoms in each ring are alternately directed toward the interior and the exterior, as in the previously cited complex⁹ and also in the hcb network displaying polycatenation recently reported.¹⁰ In contrast to the last case, the hcb layers in **3** and **4** assume a nearly flat shape and are arranged in groups of two, with the $[\text{UO}_2(\text{NMP})_2(\text{NO}_3)_2]$ units located in between, while the $[\text{M}(\text{phen})_3]_2^{2+}$ counter-ions occupy the larger spaces separating these groups. A Δ, Λ pair of

complex cations in a “phenyl embrace” arrangement³⁵ can be considered to be associated with and partly penetrates one side of each of the large rings making up the hcb structure. The packing of the sheets defines channels directed along the *c* axis which contain the counter-ions and neutral uranyl species. Several parallel-displaced π -stacking interactions may be present between either thiophene and phen rings or phen rings only, with centroid...centroid distances in the range 3.643(9)–4.496(8) Å and dihedral angles of 0–17.3(7)°. Five CH... π interactions between phen hydrogen atoms and either thiophene or phen rings may also be significant (H...centroid distances in the range 2.47–2.93 Å, C–H...centroid angles of 141–148°).

The last two complexes contain silver(I) cations and were obtained either in the absence of a chelating *N*-donor in the case of [Ag(CH₃CN)₃]₂[(UO₂)₂(TDC)₃]₂·H₂O (**5**), or in the presence of bipy in that of [Ag(bipy)₂]₅[(UO₂)₄(TDC)₆]₂·NO₃·6H₂O (**6**). Complex **5** crystallizes in the tetragonal space group *P4₂/nmc*, with the unique uranium atom located on a mirror plane (site 8g) and the silver ion on a two-fold rotation axis (site 8f), while the TDC²⁻ ligand containing S1 has twofold rotation symmetry, and that containing S2 is centered on the intersection of two mirror planes and is disordered in consequence, the two positions being only partly resolved (see Experimental). The uranium atom is chelated by three carboxylate groups (Fig. 4), with U–O(carboxylate) bond lengths in the range 2.458(5)–2.482(5) Å [average 2.472(10) Å]. This connectivity results in the formation of a 2D network parallel to the (0 0 1) plane and with the point symbol {4.8²} corresponding to the common fes topological type which results from a tessellation of 4- and 8-membered rings.³⁶ The same topology is found in the complex [(UO₂)₂(TDC)₃]₂·(6-Me-bipy)₂·5H₂O.¹⁰ In both cases, the four sulfur atoms of the 4-membered rings are all directed inward; six are pointing outward in the 8-membered rings of the previous structure, while four are pointing outward in **5**, the others being disordered. The packing of the

layers in **5** brings the 4-membered ring of one layer at the centre of the 8-membered ones of its neighbours, when viewed down the *c* axis. The disordered and very badly resolved $[\text{Ag}(\text{CH}_3\text{CN})_3]^+$ counter-ions occupy the 8-membered cavities ($[\text{Ag}(\text{CH}_3\text{CN})_x]^+$ cations with $x = 2\text{--}4$ have previously been reported³⁷). Unlike the counter cations in complexes **3** and **4**, the planar $[\text{Ag}(\text{CH}_3\text{CN})_3]^+$ cations lie essentially within the plane of the uranyl polymer sheets and can be considered a template for the larger ring formation probably involving CH...O interactions. The smaller rings accommodate water molecules. Parallel π -stacking interactions may be present between the disordered thiophene rings of adjacent layers (centroid...centroid distance ~ 3.52 Å).

Complex **6** crystallizes in the orthorhombic Sohncke group $P2_12_12_1$ and its large asymmetric unit contains four uranium atoms, all of them chelated by three carboxylate groups, six TDC^{2-} ligands, all bis-chelating, and five $[\text{Ag}(\text{bipy})_2]^+$ counter-ions (Fig. 5). The U–O(carboxylate) bond lengths are in the usual range $[2.429(8)\text{--}2.513(8)$ Å, average $2.47(2)$ Å]. A two-dimensional hcb network similar to those in complexes **3** and **4** and others previously described^{9,10} is formed. Although the $[\text{Ag}(\text{bipy})_2]^+$ units have a severely flattened tetrahedral geometry, they are clearly non-planar and this may be a factor explaining their similarity to octahedral species in inducing a hcb network of the uranyl polymer. The other cases of such a topology gave either flat layers which ran in a parallel, non-interpenetrating way, or, in one case, gently undulating sheets displaying parallel 2D \rightarrow 2D polycatenation.¹⁰ In contrast, the networks in **6** are quite flat, but they are involved in inclined 2D \rightarrow 3D polycatenation, with an angle of 60.9° between the two families of planes, parallel to $(0\ 1\ -2)$ or $(0\ 1\ 2)$ and intersecting along a line parallel to the *a* axis (Fig. 5). The size of the rings (~ 15.5 Å \times 14 Å in the largest and smallest dimensions) allows one rod of one layer to pass through one ring of the other, as in other examples of 2D \rightarrow 3D polycatenation in uranyl complexes,^{11f} while the larger size of the rings

generated in complexes with 4,4'-biphenyldicarboxylate ($\sim 27 \text{ \AA} \times 22/23 \text{ \AA}$) allows four rods to pass through each ring.⁵ The formation of this entanglement in **6** is probably directed by the $[\text{Ag}(\text{bipy})_2]^+$ counter-ions which are arranged in columns parallel to the *a* axis, i.e. the line of intersection of the 2D networks, and thus occupy the channels which run along this axis (largest and smallest dimensions of the diamond-shaped cross-section $\sim 26 \text{ \AA} \times 15 \text{ \AA}$). Unsurprisingly, many short distances between the centroids of the bipy rings, down to $3.587(9) \text{ \AA}$, indicate that parallel-displaced π -stacking interactions contribute to the cohesion of these columns. The silver ions are irregularly spaced along the column, with Ag...Ag separations of $4.527(2)$, $3.2752(19)$, $3.690(2)$, $3.785(3)$ and $3.456(3) \text{ \AA}$ (beginning with Ag1), all of them being larger than twice the van der Waals radius of silver (1.72 \AA),³⁸ but for the second, between Ag2 and Ag3, which may be indicative of a weak argentophilic interaction shown in Fig. 5; contacts shorter than 3.15 \AA are however common in comparable silver chains and distances as small as 2.72 \AA have been measured.³⁹ Several CH... π interactions may be significant, between hydrogen atoms of bipy molecules and thiophene rings (H...centroid distances in the range 2.63 – 3.00 \AA , C–H...centroid angles of 128 – 158°), although, as already stated, coulombic interactions are by far the dominant anion–cation interactions.

Luminescence Properties

Emission spectra under excitation at a wavelength of 420 nm , a value suitable for uranyl excitation and corresponding to the U=O axial LMCT band,⁴⁰ in the solid state were recorded for all compounds except **5**, for which a sufficient amount of crystals could not be isolated, and they are represented in Fig. 6. As frequently observed when 3d-block transition metal ions are present, complexes **1–4** display complete quenching of uranyl luminescence, which is attributed to energy

transfer to the d–d excited state followed by nonradiative decay.^{8,26b,c,41} Only in the case of complex **6** is a spectrum with typical uranyl emission obtained, which shows that no quenching by silver(I) ions occurs (at least in this particular instance). The vibronic progression corresponding to the $S_{11} \rightarrow S_{00}$ and $S_{10} \rightarrow S_{0\nu}$ ($\nu = 0-4$) electronic transitions⁴² appears clearly, with intense and well resolved maxima at 497 (s), 519 (s), 543 (s), 569 (m) and 597 (w) nm. These values are close to those measured in other uranyl carboxylate complexes,^{5,8,26d,41d,43} but a redshift of ~20 nm is observed with respect to the values generally observed in uranyl complexes with six carboxylate oxygen donors in the equatorial plane. This indicates that the coordination number is only one factor influencing the uranyl emission spectra, even within a family of closely related complexes, and that slight variations in the strength of the ligands are also effective.⁴⁴ The vibronic splitting energy of the $S_{10} \rightarrow S_{0\nu}$ transitions is in the range 824–853 cm^{-1} , these values being comparable to that of 852 cm^{-1} in uranyl malonates.⁴² The origin of the ill-defined and relatively weak emission in complex **2** is unknown, since complexes such as $\Lambda\text{-}[\text{Co}((\text{NH}_3)_2\text{sar})]^{5+}$ are non-luminescent but it certainly is not attributable to the uranyl centres.

Conclusions

The complexes formed by uranyl ions with 2,5-thiophenedicarboxylic acid have lately been the subject of several reports from which it appears that the use of various additional species, be they co-ligands, co-solvents, guest species or counter-ions, results in a wide variety of dimensionalities, from 0D to 3D, and of topologies in the case of the polymeric assemblies.⁷⁻¹⁰ The present work is part of an ongoing investigation of the effect of the presence of d-block metal-containing counterions on the nature and geometry of the uranyl ion complexes formed with common polycarboxylates. The $[\text{M}(\text{bipy}/\text{phen})_x]^{n+}$ ($x = 2$ or 3 , $n = 1$ or 2) counter-ions are

particularly appealing in this context, and $[\text{Ni}(\text{bipy})_3]^{2+}$, $[\text{Ni}(\text{phen})_3]^{2+}$, $[\text{Fe}(\text{phen})_3]^{2+}$ and $[\text{Ag}(\text{bipy})_2]^+$ were used in the present work, as well as the enantiomerically pure Λ - $[\text{Co}((\text{NH}_2)_2\text{sar})]^{3+}$. One complex was also obtained with Ag^+ cations in the absence of a chelating *N*-donor. In all cases, the uranyl ions are tris-chelated by three carboxylate groups (one of them replaced by a nitrate ion in one instance), and the ligands are either fully deprotonated and bis-chelating, or they retain an uncoordinated carboxylic group. When at least one terminal HTDC^- ligand is present, the complex crystallizes as a planar, zigzag-shaped 1D coordination polymer, whereas in all the other cases 2D assemblies are formed. The latter assume either the hcb $\{6^3\}$ or the fes $\{4.8^2\}$ topological types. In one of the hcb species, the flat layers are polycatenated to give a 3D architecture; the structure-directing role exerted by the counter-ions is particularly apparent here since the intersecting layers define channels containing columns of $[\text{Ag}(\text{bipy})_2]^+$ cations held together by π -stacking and weak argentophilic interactions. This last complex only displays typical uranyl ion emission in the solid state, luminescence quenching being nearly complete in all the other compounds. The most important interaction between the various cations and the uranyl polymers appears to be of the type $\text{CH}\cdots\text{O}$, although for the bipy and phen complexes there appear to be subtle differences relating to whether the oxygen centre comes from uranyl or a ligand (carboxylate or nitrate).

References

1. For a general overview of metal–organic frameworks (MOFs), see: (a) T. R. Cook, Y. R. Zheng and P. J. Stang, *Chem. Rev.*, 2013, **113**, 734; (b) H. Furukawa, K. E. Cordova, M. O’Keeffe and O. M. Yaghi, *Science*, 2013, **341**, 1230444.
2. For an overview of uranyl–organic coordination polymers and frameworks, see: (a) C. L. Cahill, D. T. de Lill and M. Frisch, *CrystEngComm*, 2007, **9**, 15; (b) C. L. Cahill and L. A. Borkowski, in *Structural Chemistry of Inorganic Actinide Compounds*; S. V. Krivovichev, P. C. Burns and I. G. Tananaev, Eds.; Elsevier, Amsterdam, Oxford, 2007, ch. 11; (c) K. X. Wang and J. S. Chen, *Acc. Chem. Res.*, 2011, **44**, 531; (d) M. B. Andrews and C. L. Cahill, *Chem. Rev.*, 2013, **113**, 1121; (e) T. Loiseau, I. Mihalcea, N. Henry and C. Volkringer, *Coord. Chem. Rev.*, 2014, **266–267**, 69; (f) J. Su and J. S. Chen, *Struct. Bond.*, 2015, **163**, 265.
3. (a) S. Kitagawa, R. Kitaura and S. I. Noro, *Angew. Chem. Int. Ed.*, 2004, **43**, 2334; (b) P. Pachfule, C. Dey, T. Panda and R. Banerjee, *CrystEngComm*, 2010, **12**, 1600.
4. P. Thuéry and J. Harrowfield, *Inorg. Chem.*, 2015, **54**, 10539.
5. P. Thuéry and J. Harrowfield, *Inorg. Chem.*, 2015, **54**, 8093.
6. (a) F. H. Allen, *Acta Crystallogr., Sect. B*, 2002, **58**, 380; (b) I. J. Bruno, J. C. Cole, P. R. Edgington, M. Kessler, C. F. Macrae, P. McCabe, J. Pearson and R. Taylor, *Acta Crystallogr., Sect. B*, 2002, **58**, 389.
7. S. G. Thangavelu, M. B. Andrews, S. J. A. Pope and C. L. Cahill, *Inorg. Chem.*, 2013, **52**, 2060.
8. P. Thuéry and J. Harrowfield, *Cryst. Growth Des.*, 2014, **14**, 1314.
9. H. H. Li, X. H. Zeng, H. Y. Wu, X. Jie, S. T. Zheng and Z. R. Chen, *Cryst. Growth Des.*, 2015, **15**, 10.

10. S. G. Thangavelu, R. J. Butcher and C. L. Cahill, *Cryst. Growth Des.*, 2015, **15**, 3481.
11. (a) L. A. Borkowski and C. L. Cahill, *Cryst. Growth Des.*, 2006, **6**, 2248; (b) Y. B. Go, X. Wang and A. J. Jacobson, *Inorg. Chem.*, 2007, **46**, 6594; (c) S. Lis, Z. Glatty, G. Meinrath and M. Kubicki, *J. Chem. Crystallogr.*, 2010, **40**, 646; (d) H. Y. Wu, R. X. Wang, W. Yang, J. Chen, Z. M. Sun, J. Li and H. Zhang, *Inorg. Chem.*, 2012, **51**, 3103; (e) F. Chen, C. Z. Wang, Z. J. Li, J. H. Lan, Y. Q. Ji and Z. F. Chai, *Inorg. Chem.*, 2015, **54**, 3829; (f) Y. Wang, Z. Liu, Y. Li, Z. Bai, W. Liu, Y. Wang, X. Xu, C. Xiao, D. Sheng, J. Diwu, J. Su, Z. Chai, T. E. Albrecht-Schmitt and S. Wang, *J. Am. Chem. Soc.*, 2015, **137**, 6144; (g) L. Mei, Q. Y. Wu, S. W. An, Z. Q. Gao, Z. F. Chai and W. Q. Shi, *Inorg. Chem.*, 2015, **54**, 10934.
12. V. M. Russell, M. L. Scudder and I. G. Dance, *J. Chem. Soc., Dalton Trans.*, 2001, 789.
13. R. Puttreddy, Y. Gorodetski, J. M. Harrowfield, J. A. Hutchison and K. Rissanen, *Cryst. Growth Des.*, 2015, **15**, 1559 and references therein.
14. I. J. Clark, A. Crispini, P. S. Donnelly, L. M. Engelhardt, J. M. Harrowfield, S. H. Jeong, Y. Kim, G. A. Koutsantonis, Y. H. Lee, N. A. Lengkeek, M. Mocerino, G. L. Nealon, M. I. Ogden, Y. C. Park, C. Pettinari, L. Polanzan, E. Rukmini, A. M. Sargeson, B. W. Skelton, A. N. Sobolev, P. Thuéry and A. H. White, *Aust. J. Chem.*, 2009, **62**, 1246.
15. S. Eckhardt, P. S. Brunetto, J. Gagnon, M. Priebe, B. Giese and K. M. Fromm, *Chem. Rev.*, 2013, **113**, 4708.
16. H. Akdas, E. Graf, M. W. Hosseini, A. De Cian and J. M. Harrowfield, *Chem. Commun.*, 2000, 2219 and references therein.
17. L. A. Lednický and D. M. Stanbury, *J. Am. Chem. Soc.*, 1983, **105**, 3098.
18. R. J. Geue, T. W. Hambley, J. M. Harrowfield, A. M. Sargeson and M. R. Snow, *J. Am. Chem. Soc.*, 1984, **106**, 5478.

19. R. W. W. Hoof, *COLLECT*; Nonius BV: Delft, The Netherlands, 1998.
20. Z. Otwinowski and W. Minor, *Methods Enzymol.*, 1997, **276**, 307.
21. G. M. Sheldrick, *Acta Crystallogr., Sect. A*, 2015, **71**, 3.
22. (a) G. M. Sheldrick, *Acta Crystallogr., Section A*, 2008, **64**, 112; (b) G. M. Sheldrick, *Acta Crystallogr., Sect. C*, 2015, **71**, 3.
23. L. J. Farrugia, *J. Appl. Crystallogr.*, 1997, **30**, 565.
24. K. Momma and F. Izumi, *J. Appl. Crystallogr.*, 2008, **41**, 653.
25. (a) V. A. Blatov, A. P. Shevchenko and V. N. Serezhkin, *J. Appl. Crystallogr.*, 2000, **33**, 1193; (b) V. A. Blatov, M. O'Keeffe and D. M. Proserpio, *CrystEngComm*, 2010, **12**, 44.
26. (a) P. Thuéry, *Cryst. Growth Des.*, 2014, **14**, 901; (b) P. Thuéry and J. Harrowfield, *CrystEngComm*, 2014, **16**, 2996; (c) P. Thuéry, E. Rivière and J. Harrowfield, *Inorg. Chem.*, 2015, **54**, 2838; (d) P. Thuéry and J. Harrowfield, *CrystEngComm*, 2015, **17**, 4006.
27. A. Gavezzotti, *CrystEngComm*, 2013, **15**, 4027.
28. (a) K. S. C. Reid, P. F. Lindley and J. M. Thornton, *FEBS Lett.*, 1985, **190**, 209; (b) S. Yan, S. J. Lee, S. Kang, K. H. Choi, S. K. Rhee and J. Y. Lee, *Bull. Korean Chem. Soc.*, 2007, **28**, 959.
29. (a) M. E. Brezgunova, J. Lieffrig, E. Aubert, S. Dahaoui, P. Fertey, S. Lebègue, J. G. Ángyán, M. Fourmigué and E. Espinosa, *Cryst. Growth Des.*, 2013, **13**, 3283; (b) M. Bai, S. P. Thomas, R. Kottokkaran, S. K. Nayak, P. C. Ramamurthy and T. N. Guru Row, *Cryst. Growth Des.*, 2014, **14**, 459.
30. (a) J. J. McKinnon, A. S. Mitchell and M. A. Spackman, *Chem.–Eur. J.*, 1998, **4**, 2136; (b) M. A. Spackman and J. J. McKinnon, *CrystEngComm*, 2002, **4**, 378; (c) J. J. McKinnon, M. A. Spackman and A. S. Mitchell, *Acta Crystallogr., Sect. B*, 2004, **60**, 627; (d) J. J. McKinnon, D.

- Jayatilaka and M. A. Spackman, *Chem. Commun.*, 2007, 3814; (e) M. A. Spackman and D. Jayatilaka, *CrystEngComm*, 2009, **11**, 19; (f) M. A. Spackman, *Phys. Scr.*, 2013, **87**, 048103 (12 pp).
31. S. K. Wolff, D. J. Grimwood, J. J. McKinnon, M. J. Turner, D. Jayatilaka and M. A. Spackman, *CrystalExplorer*, University of Western Australia, 2012.
32. (a) R. Taylor and O. Kennard, *J. Am. Chem. Soc.*, 1982, **104**, 5063; (b) G. R. Desiraju, *Acc. Chem. Res.*, 1991, **24**, 290; (c) G. R. Desiraju, *Acc. Chem. Res.*, 1996, **29**, 441.
33. P. Thuéry, *Inorg. Chem. Commun.*, 2015, **59**, 25.
34. A. L. Spek, *J. Appl. Crystallogr.*, 2003, **36**, 7.
35. V. Russell, M. Scudder and I. Dance, *J. Chem. Soc., Dalton Trans.*, 2001, 789 and references therein.
36. V. A. Blatov and D. M. Proserpio, in *Modern Methods of Crystal Structure Prediction*, A. R. Oganov, Ed.; Wiley-VCH, Weinheim, Germany, 2011.
37. (a) Y. Zhang, A. M. Santos, E. Herdtweck, J. Mink and F. E. Kühn, *New J. Chem.*, 2005, **29**, 366; (b) J. K. Jabor, R. Stößer, N. H. Thong, B. Ziemer and M. Meisel, *Angew. Chem. Int. Ed.*, 2007, **46**, 6354; (c) C. Wölper, A. Rodríguez-Gimeno, K. Chulvi Iborra, H. Kuhn, A. K. Lüttig, S. Moll, C. Most, M. Freytag, I. Dix, P. G. Jones and A. Blaschette, *Z. Naturforsch.*, 2009, **64b**, 952.
38. A. Bondi, *J. Phys. Chem.*, 1964, **68**, 441.
39. M. J. Hannon, C. L. Painting, E. A. Plummer, L. J. Childs and N. W. Alcock, *Chem.–Eur. J.*, 2002, **8**, 2226.

40. (a) K. E. Knope, D. T. de Lill, C. E. Rowland, P. M. Cantos, A. de Bettencourt-Dias and C. L. Cahill, *Inorg. Chem.*, 2012, **51**, 201; (b) S. G. Thangavelu and C. L. Cahill, *Cryst. Growth Des.*, 2016, **16**, 42.
41. (a) A. N. Alsobrook, W. Zhan and T. E. Albrecht-Schmitt, *Inorg. Chem.*, 2008, **47**, 5177; (b) J. Heine and K. Müller-Buschbaum, *Chem. Soc. Rev.*, 2013, **42**, 9232; (c) A. T. Kerr and C. L. Cahill, *Cryst. Growth Des.*, 2014, **14**, 1914; (d) P. Thuéry and J. Harrowfield, *Inorg. Chem.*, 2015, **54**, 6296.
42. A. Brachmann, G. Geipel, G. Bernhard and H. Nitsche, *Radiochim. Acta*, 2002, **90**, 147.
43. P. Thuéry, B. Masci and J. Harrowfield, *Cryst. Growth Des.*, 2013, **13**, 3216.
44. (a) M. P. Redmond, S. M. Cornet, S. D. Woodall, D. Whittaker, D. Collison, M. Helliwell and L. S. Natrajan, *Dalton Trans.*, 2011, **40**, 3914; (b) K. P. Carter, M. Kalaj and C. L. Cahill, *Eur. J. Inorg. Chem.*, 2016, 126.

Table 1 Crystal data and structure refinement details

	1	2	3	4	5	6
Chemical formula	C ₅₃ H ₄₂ N ₈ NiO ₂₁ S ₃ U ₂	C ₃₈ H ₅₆ ClCoN ₈ O ₂₆ S ₄ U ₂	C ₁₂₈ H ₉₆ Fe ₂ N ₁₈ O ₄₄ S ₆ U ₅	C ₁₂₃ H ₈₇ N ₁₇ Ni ₂ O ₄₃ S ₆ U ₅	C ₃₀ H ₂₆ Ag ₂ N ₆ O ₁₇ S ₃ U ₂	C ₁₃₆ H ₁₀₄ Ag ₅ N ₂₁ O ₄₁ S ₆ U ₄
<i>M</i> /g mol ⁻¹	1757.89	1739.58	4084.43	3991.02	1530.55	4372.23
Crystal system	Triclinic	Monoclinic	Triclinic	Triclinic	Tetragonal	Orthorhombic
Space group	<i>P</i> $\bar{1}$	<i>P</i> 2 ₁	<i>P</i> $\bar{1}$	<i>P</i> $\bar{1}$	<i>P</i> 4 ₂ / <i>nnc</i>	<i>P</i> 2 ₁ 2 ₁
<i>a</i> /Å	13.8935(5)	10.8016(4)	13.7311(8)	13.7804(3)	26.1007(3)	18.4849(2)
<i>b</i> /Å	14.0662(8)	20.4090(8)	15.5105(9)	15.5944(3)	26.1007(3)	26.8834(6)
<i>c</i> /Å	18.2195(11)	12.8547(5)	17.8862(9)	18.0932(4)	6.6950(2)	31.5917(8)
α /°	108.577(2)	90	68.574(3)	67.6388(9)	90	90
β /°	110.263(3)	105.973(2)	70.094(3)	69.3880(9)	90	90
γ /°	97.592(3)	90	76.948(3)	76.7394(11)	90	90
<i>V</i> /Å ³	3046.3(3)	2724.41(18)	3311.7(3)	3345.09(13)	4560.95(17)	15699.1(6)
<i>Z</i>	2	2	1	1	4	4
<i>D</i> _{calcd} /g cm ⁻³	1.916	2.121	2.048	1.981	2.229	1.850
μ (Mo K α)/mm ⁻¹	5.793	6.525	6.492	6.488	8.134	4.881
<i>F</i> (000)	1688	1680	1950	1900	2840	8376
Reflections collected	171362	101930	156076	211033	101372	327711
Independent reflections	11564	10337	12556	12668	2263	29722
Observed reflections [<i>I</i> > 2 σ (<i>I</i>)]	9122	9510	10361	11466	1989	24835
<i>R</i> _{int}	0.057	0.029	0.049	0.040	0.012	0.034
Parameters refined	812	731	918	918	174	1910
<i>R</i> ₁	0.033	0.034	0.052	0.069	0.039	0.045
<i>wR</i> ₂	0.093	0.119	0.144	0.190	0.102	0.111
<i>S</i>	1.069	1.073	1.027	1.094	1.084	1.034
$\Delta\rho_{\min}$ /e Å ⁻³	-1.67	-1.32	-6.56	-9.09	-1.29	-0.90
$\Delta\rho_{\max}$ /e Å ⁻³	1.74	1.71	1.49	1.81	1.38	1.02

Figure Captions

Fig. 1 Top: View of complex **1**. Displacement ellipsoids are drawn at the 40% probability level. The water solvent molecule and the carbon-bound hydrogen atoms are omitted. The hydrogen bond is shown as a dashed line. Symmetry codes: $i = x + 1, y + 1, z$; $j = x - 1, y - 1, z$. Middle: View of the 1D assembly. Bottom: View of the packing with chains viewed end-on; solvent molecules and hydrogen atoms are omitted. The uranium coordination polyhedra are colored yellow and those of nickel green.

Fig. 2 Top left: View of complex **2**. Displacement ellipsoids are drawn at the 50% probability level. Chlorine counter-ions, solvent molecules and carbon-bound hydrogen atoms are omitted. Hydrogen bonds are shown as dashed lines. Symmetry codes: $i = x - 1, y, z + 1$; $j = x + 1, y, z - 1$. Top right: View of two chains and cobalt-containing counterions in one layer. Bottom left: View of two layers and the imbedded cobalt-containing counter-ions. Bottom right: View of the packing with solvent molecules and hydrogen atoms omitted; chlorine atoms are shown as green spheres.

Fig. 3 Top: View of complex **4** (isomorphous with complex **3**). Displacement ellipsoids are drawn at the 30% probability level. Symmetry codes: $i = x, y - 1, z + 1$; $j = x + 1, y, z - 1$; $k = x - 1, y, z + 1$; $l = x, y + 1, z - 1$; $m = -x, -y, 1 - z$. Middle: View of the 2D assembly and the neutral uranyl-containing complexes. Bottom: View of the packing with layers viewed edge-on. The uranium coordination polyhedra are colored yellow and those of nickel green. Solvent molecules and hydrogen atoms are omitted in all views.

Fig. 4 Top: View of complex **5**. Displacement ellipsoids are drawn at the 40% probability level and only one position of the disordered ligand is represented. Symmetry codes: $i = 3/2 - x, y, z$; $j = 1 - y, 1 - x, 3/2 - z$; $k = x, 3/2 - y, z$. Middle: View of the 2D assembly. Bottom: View of the packing with layers viewed face-on. The uranium coordination polyhedra are colored yellow and silver ions are represented as dark blue spheres; disordered atoms are shown as parti-colored spheres. Solvent molecules and hydrogen atoms are omitted in all views.

Fig. 5 Top left: View of complex **6**. Displacement ellipsoids are drawn at the 30% probability level. Symmetry codes: $i = x - 1/2, 3/2 - y, 1 - z$; $j = x + 1, y, z$; $k = x + 1/2, -y - 1/2, -z$; $l = x + 1/2, 3/2 - y, 1 - z$; $m = x - 1, y, z$; $n = x - 1/2, -y - 1/2, -z$. Top right: Two intersecting 2D networks (the parts below the intersection line are not shown for clarity). Bottom left: The polycatenated assembly with sheets viewed edge-on and silver-containing columns viewed end-on. The nitrate counter-ions, water solvent molecules and hydrogen atoms are omitted in all views. Bottom right: Nodal representation of the polycatenated networks.

Fig. 6 Solid state emission spectra of complexes **1–4** and **6**. Excitation wavelength 420 nm.

Figure 1

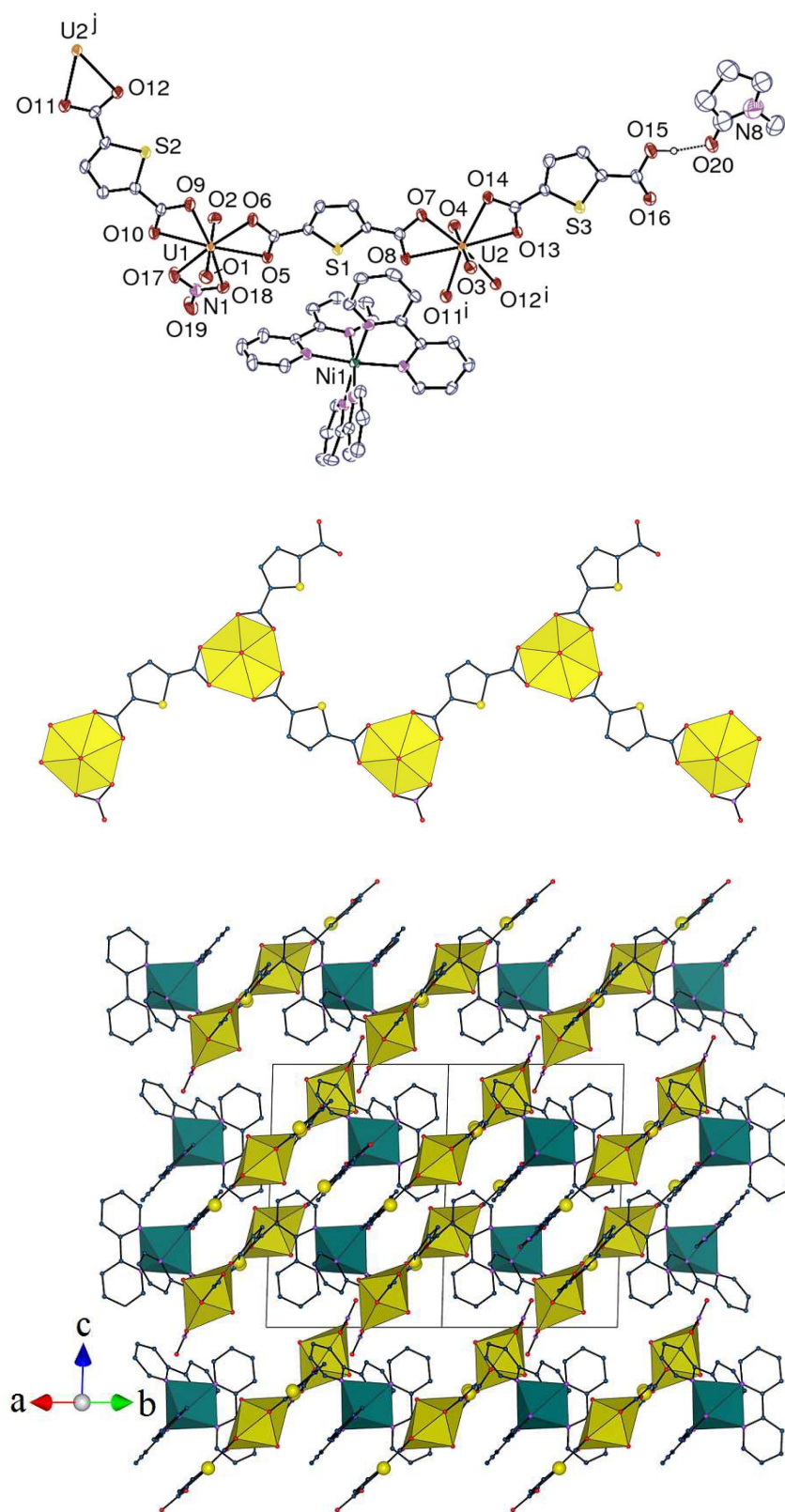


Figure 2

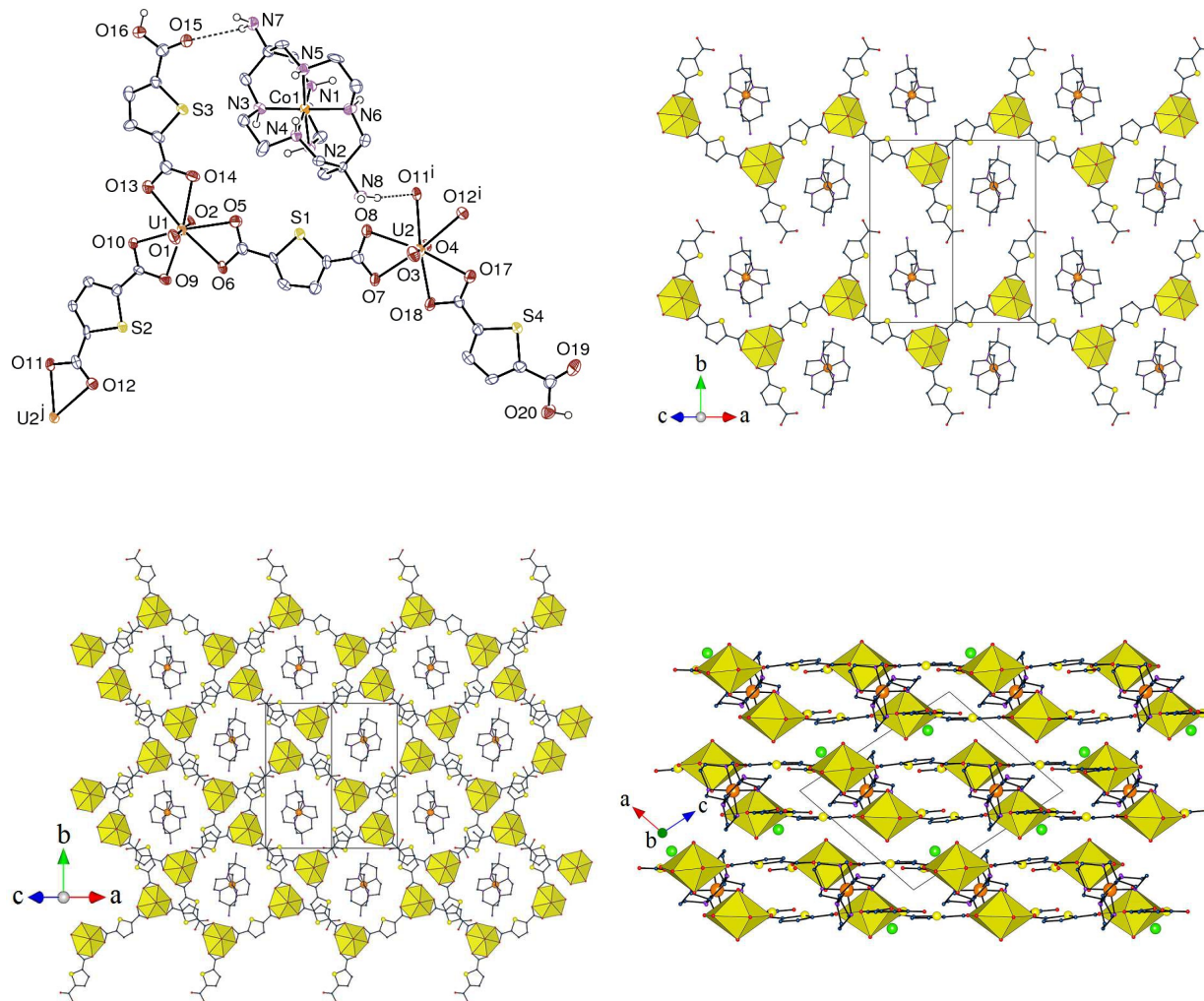


Figure 3

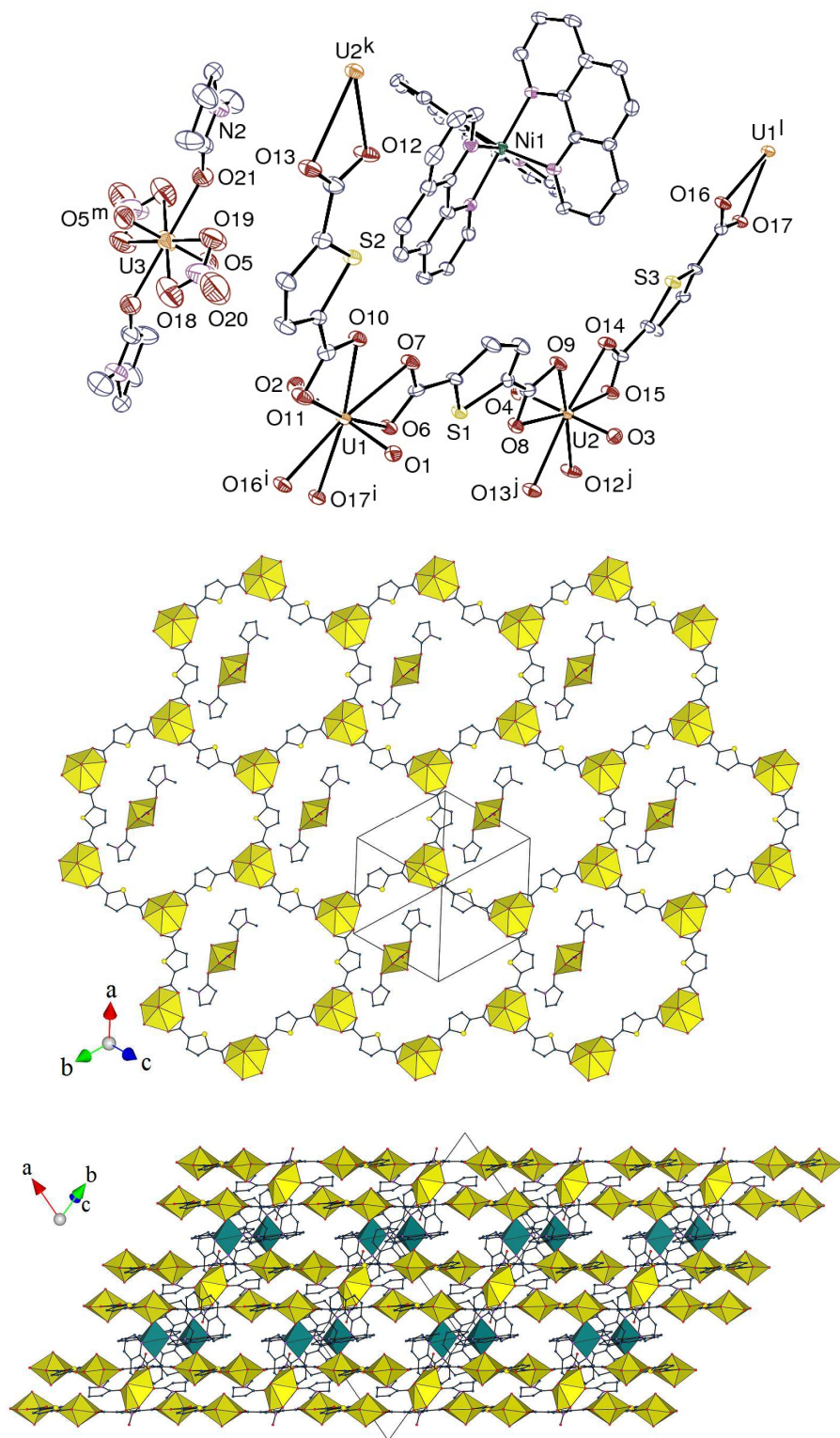


Figure 4

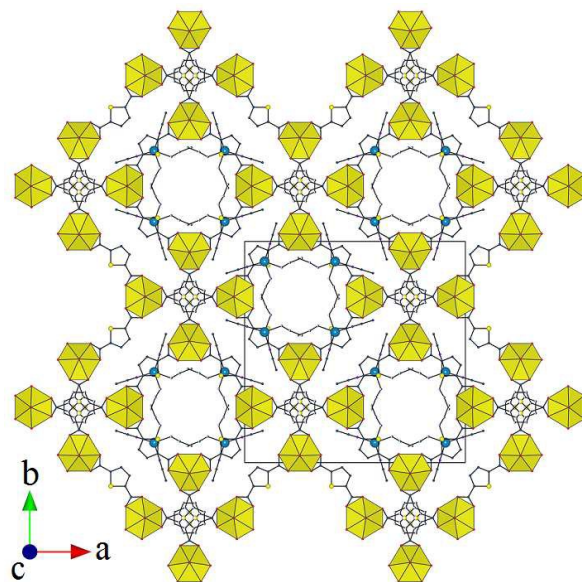
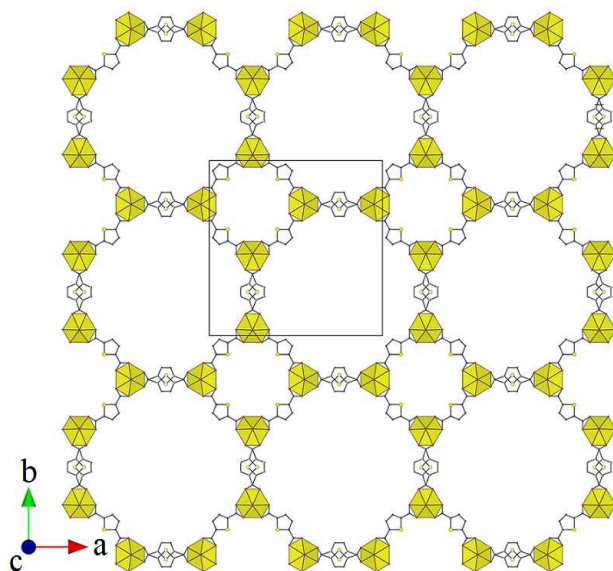
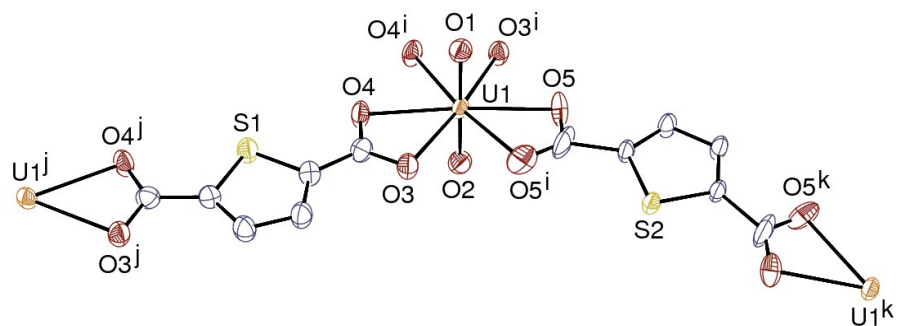


Figure 5

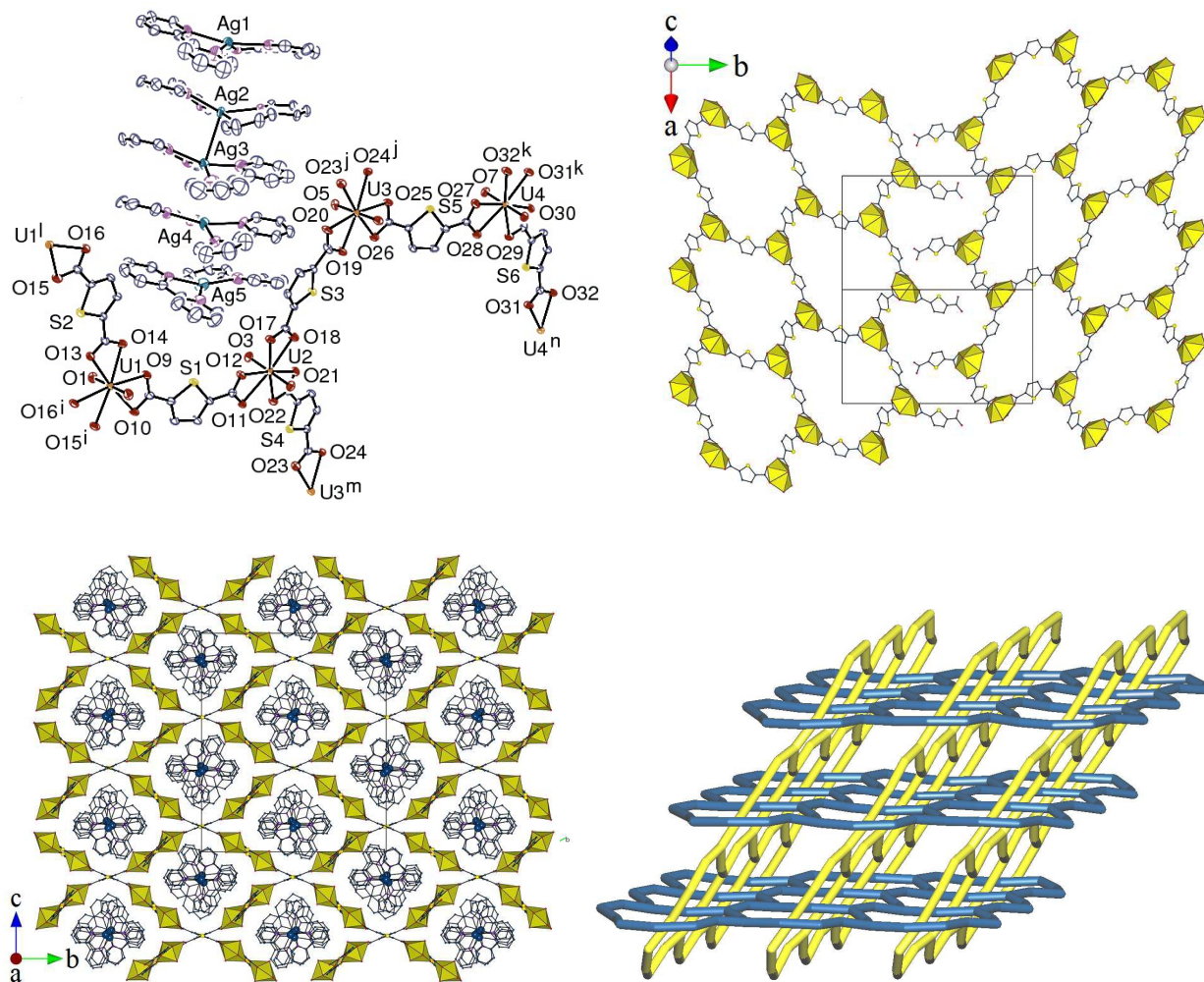
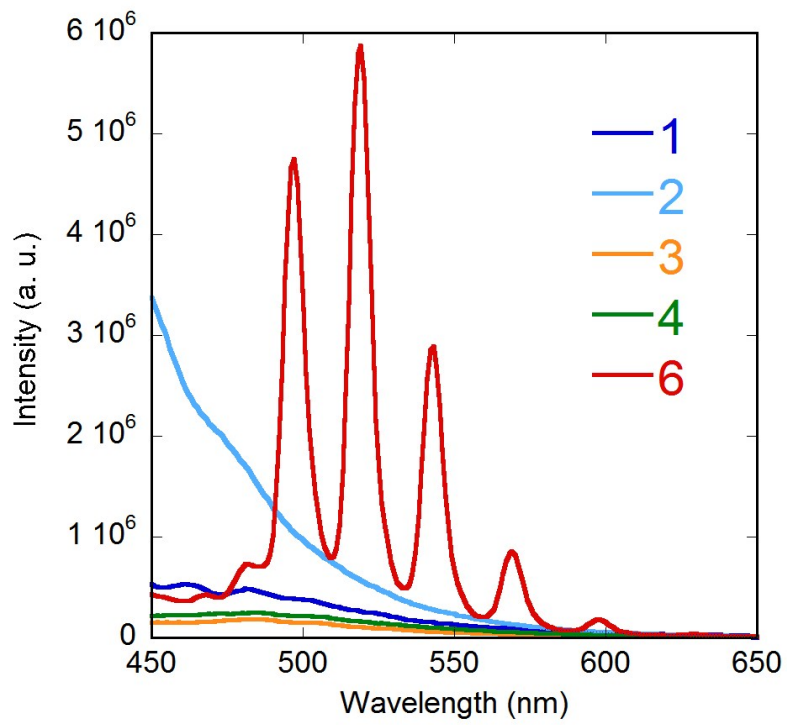


Figure 6



For Table of Contents Use Only

Counter-ion control of structure in uranyl ion complexes with 2,5-thiophenedicarboxylate

Pierre Thuéry and Jack Harrowfield

Various counterions containing d-block metal ions and *N*-donating chelators were used to generate one- and two-dimensional uranyl–2,5-thiophenedicarboxylate species, one of them displaying inclined polycatenation.

